

# Ionic Modification Turns Commercial Rubber into a Self-Healing Material

Amit Das,<sup>\*,†,‡</sup> Aladdin Sallat,<sup>†,§</sup> Frank Böhme,<sup>†</sup> Marcus Suckow,<sup>†,§</sup> Debdipta Basu,<sup>†,§</sup> Sven Wießner,<sup>†,§</sup> Klaus Werner Stöckelhuber,<sup>†</sup> Brigitte Voit,<sup>†,§</sup> and Gert Heinrich<sup>†,§</sup>

<sup>†</sup>Leibniz-Institut für Polymerforschung Dresden e.V., D-01069 Dresden, Germany

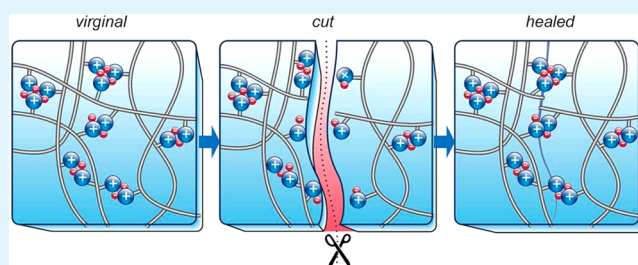
<sup>‡</sup>Tampere University of Technology, FI-33101, Tampere, Finland

<sup>§</sup>Technische Universität Dresden, D-01062 Dresden, Germany

## S Supporting Information

**ABSTRACT:** Invented by Charles Goodyear, chemical cross-linking of rubbers by sulfur vulcanization is the only method by which modern automobile tires are manufactured. The formation of these cross-linked network structures leads to highly elastic properties, which substantially reduces the viscous properties of these materials. Here, we describe a simple approach to converting commercially available and widely used bromobutyl rubber (BIIR) into a highly elastic material with extraordinary self-healing properties without using conventional cross-linking or vulcanising agents. Transformation of the bromine functionalities of BIIR into ionic imidazolium bromide groups results in the formation of reversible ionic associates that exhibit physical cross-linking ability. The reversibility of the ionic association facilitates the healing processes by temperature- or stress-induced rearrangements, thereby enabling a fully cut sample to retain its original properties after application of the self-healing process. Other mechanical properties, such as the elastic modulus, tensile strength, ductility, and hysteresis loss, were found to be superior to those of conventionally sulfur-cured BIIR. This simple and easy approach to preparing a commercial rubber with self-healing properties offers unique development opportunities in the field of highly engineered materials, such as tires, for which safety, performance, and longer fatigue life are crucial factors.

**KEYWORDS:** self-healing, elastomers, ionic associations, bromobutyl rubbers, network structures



## INTRODUCTION

Inspired by nature, scientists have long been motivated to develop self-healing materials. As a result, various types of self-healing materials, ranging from solid concrete to soft elastomers, have been introduced.<sup>1–15</sup> Some of the reported materials exhibit excellent mechanical properties, repeatable self-healing, and easy processability, particularly when a supramolecular assembly approach was followed.<sup>2</sup>

In the field of elastomers, Leibler et al.'s pioneering work<sup>2</sup> provided decisive motivation for developing new rubber materials with self-healing behavior. The authors described a supramolecular rubber based on simple low-molecular-weight compounds such as fatty diacids and triacids. These compounds associate with one another to form both long chains and cross-links across the chains mainly by hydrogen bonding. This system achieves recoverable extension to several hundred percent and exhibits pronounced self-healing behavior. However, despite these promising results, doubts remain about the long-term stability of this associated network. The tire and rubber industries require up-scalable materials with a long service life and very stable and robust mechanical properties under different weather and environmental conditions. From this viewpoint, focusing our efforts on the

development of a well-established rubber by equipping it with self-healing behavior seemed to be a reasonable approach. Here, commercially available bromobutyl rubber (BIIR) exhibited very promising behavior. The ability of BIIR to react with various amines (e.g., alkyl imidazole) allows ionic functional groups to be introduced in a very simple way.<sup>16</sup> In thermoplastics, ionic groups containing polymers have already been demonstrated to exhibit self-healing behavior. A few recent studies dealt with the self-healing aspects of elastomers and showed how noncovalent interactions played a major role in demonstrating such behavior.<sup>2,17–20</sup> Besides hydrogen bonding<sup>2,20</sup> and self-adhesion,<sup>18</sup> ionic interactions<sup>17,19</sup> were assumed to be responsible for the self-healing behavior observed. Commercialization of self-healing ionomers has also been realized of late where Kalista et al.<sup>21</sup> and Varley et al.<sup>22</sup> extensively reviewed the potential aspect of self-healing ionomers based on Surllyn, a DuPont product, a neutralized copolymer of ethylene and methacrylic acid. However, modification of commercially available butyl rubber into a

Received: June 8, 2015

Accepted: September 2, 2015

Published: September 2, 2015

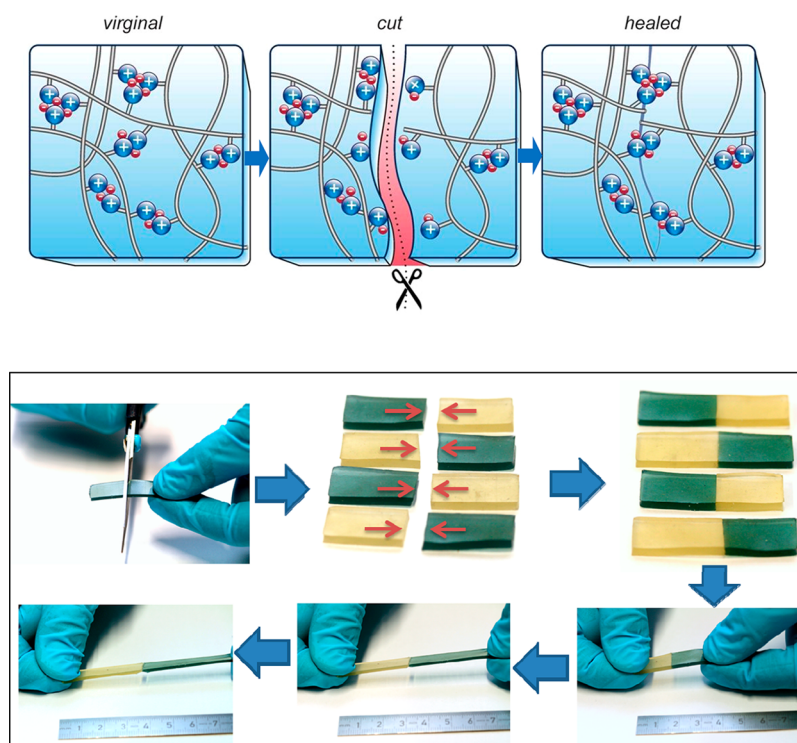


**Figure 1.** Ionic association and self-healing. (Top) Schematic representation of self-healing by reformation of ionic associates in an ionic rubber network. (Bottom) A sample of imidazolium-modified bromobutyl rubber was cut into two pieces. After reassembling and 18 h of healing time, the sample was stretched to breakdown. For better visualization, one part of the cut sample was colored.

self-healing product by simple ionic transformation has not been reported before. Moreover, the cross-linked character of the modified rubber without using any conventional curatives is first time reported here.

The aim of this study is to produce an imidazolium-modified BIIR that forms a cross-linked network by ionic association; as a result of this association, the rubber matrix becomes highly elastic. In addition, although no extra cross-linking ingredients such as sulfur or peroxides are required, the properties of this ionically modified BIIR are superior to those of conventionally cross-linked rubber. Tensile strength up to 9 MPa at a fracture elongation of 1000% was obtained.

## EXPERIMENTAL SECTION

The bromobutyl rubber (BIIR) used in this study is a commercial product of Lanxess. The bromine content was determined to be 1.13 wt % ( $^1\text{H}$  NMR), which corresponds to a brominated isoprene unit content of approximately 0.80 mol %. Butylimidazole (98%), magnesium oxide, stearic acid, sulfur, zinc oxide, and 2-mercaptobenzothiazole were purchased from Sigma-Aldrich and used without further purification.

The curing experiments were performed on mixtures consisting of 50 g of BIIR and 1.42 g (1.5 mL) g of butylimidazole in a moving die rheometer (MDR Scarabeaus SIS-V-50) at temperatures between 80 and 160 °C. The composition of the mixture corresponds to ~65% excess butylimidazole compared with the number of bromine groups. Before the measurements were taken, the components were premixed in an internal mixer (Thermo Haake Rheocord PolyLab 300p) for 10 min with a rotor speed of 60 rpm at 40 °C. During the curing process, the measurements were carried out at a sinusoidal strain of 7% with an amplitude of 0.5° and a frequency of 1.67 Hz.

For comparison, sulfur cross-linking was performed at 160 °C following a conventional compounding recipe for BIIR. In this mix, the composition was as follows: magnesium oxide, 0.5 phr; stearic acid, 1 phr; sulfur, 0.5 phr; zinc oxide, 3 phr; and 2-mercaptobenzothiazole, 1.5

phr. For the preparation of the sulfur vulcanised sample, the components were premixed in an internal mixer (Haake Rheomix, Thermo Electron GmbH, Karlsruhe, Germany) for 10 min with a rotor speed of 60 rpm at 40 °C. After that, the compounded mass was homogenized by a laboratory size two-roll mixing mill (Polymix 110L, size 203 × 102 mm, Servitech GmbH, Wustermark, Germany) for two min and then vulcanized under pressure at 160 °C. The sample obtained resembles very much a commercial rubber and served as reference to the butylimidazole modified BIIR.

$^1\text{H}$  NMR (nuclear magnetic resonance, 500.13 MHz) spectra were recorded on an Advance III 500 NMR spectrometer (Bruker).  $\text{CDCl}_3$  ( $\delta(^1\text{H}) = 7.26$  ppm) was used as the solvent and internal standard.

DSC (differential scanning calorimetry) measurements were performed on a TA Instruments Q1000. The measurements were carried out in a temperature range of -85 to 180 °C at a scanning rate of  $\pm 10$  K/min under a nitrogen atmosphere.

For the preparation of the test specimens, the premixed components were allowed to cross-link during compression molding at 100 °C for 10 min at a pressure of 10 MPa. From the obtained sheets (2 mm), test specimens with the dimensions of 35 × 10 × 2 mm were punched out.

A dynamic mechanical thermal spectrometer (EPLEXOR 2000N) from GABO QUALIMETER was used to evaluate the dynamic properties. The measurements were carried out in a temperature range of -80 to +140 °C with a heating rate of 2 K/min at a frequency of 10 Hz under 0.5% (dynamic) and 1% (static) strain.

The master curves were evaluated on the basis of the combined temperature/frequency sweep measurements from -80 to +140 °C at 0.5 to 30 Hz using the Eplexor-DMTS master curve software module. To generate the master curves, the measured frequency points were horizontally shifted according to the WLF model for a reference temperature of 20 °C.

Tensile tests were carried out on a Zwick 1456 tensile tester according to DIN EN ISO 527-2/S2/200.

BIIR, BIIR-i and BIIR-s were subjected to a tear fatigue analysis (TFA). Details of the tear fatigue analyzer and the evaluation method have been previously published.<sup>23,24</sup> In this method, the crack growth

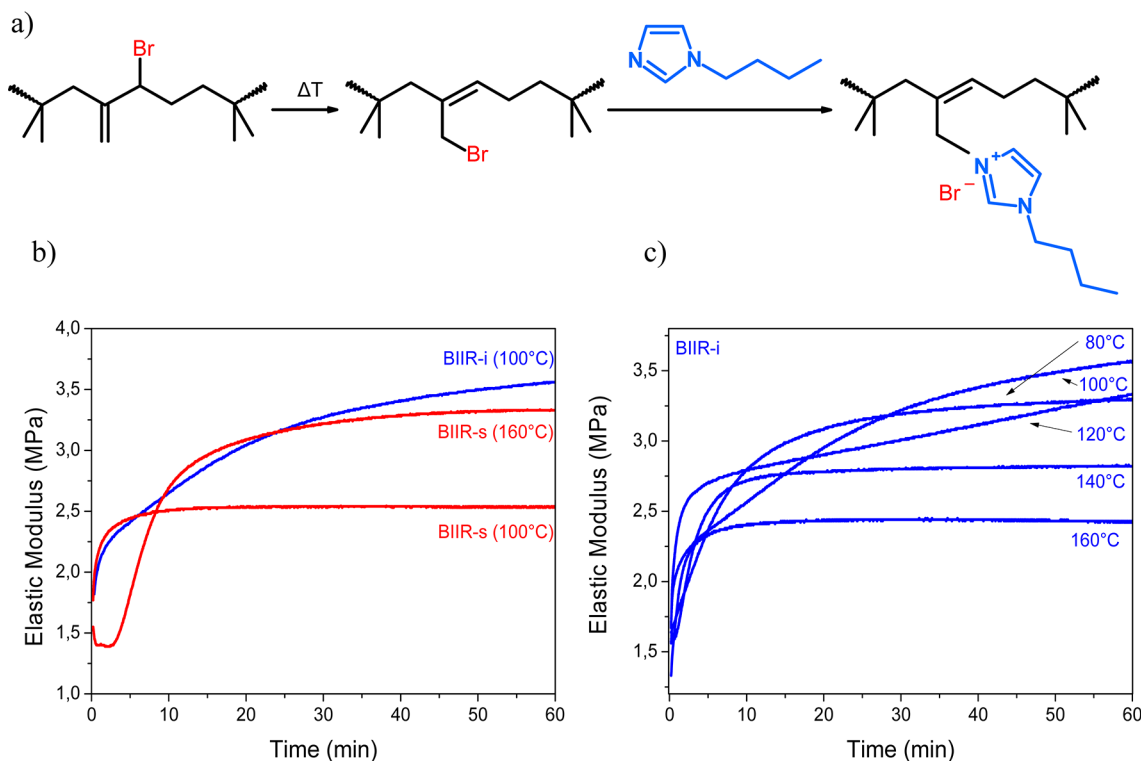


**Figure 2.** Ionic cross-linking of BIIR. (a) Reaction scheme for the conversion of BIIR with butylimidazole. (b) The course of reaction was followed on the basis of the elastic modulus measured in a moving die rheometer. The curing behaviors of imidazole (BIIR-i, blue) and sulfur (BIIR-s, red) cross-linked BIIR were compared. (c) Curing behavior of the imidazole cross-linked BIIR at different temperatures.

rate was measured in the stable crack propagation regime using pure shear specimens to avoid influence from different fracture mechanical parameters on the crack length. The crack propagation rate ( $da/dn$ , where  $a$  is the crack length and  $n$  is the number of deformation cycles) was measured at different tearing energies ( $T$ ) released per unit area by the advancing crack. The tests were performed with three pure-shear test specimens for each material. Two of them were notched on both sides, and a third specimen was left unnotched to determine the strain energy density from the cyclic stress–strain curves. All the samples were subjected to simultaneous examination under pulsed exposure (Gauß pulse: pulse width, 20 ms; pulse rate, 4 Hz) at different deformation amplitudes (13, 16, 20, and 30% of the original length) to determine the various tearing energies ( $T$ ). Optical recording and video documentation of the propagation of the crack allows for the determination of the crack growth rate ( $da/dn$ ). The obtained results were plotted as a Paris-Erdogan plot.

## RESULTS AND DISCUSSION

The ionic nature of the network facilitates segment rearrangements that may induce healing after material damage (Figure 1). Typically, butyl rubber, a random copolymer consisting of isobutylene and a small percentage of isoprene is cross-linked using elemental sulfur along with other supporting curatives. However, the cross-linking efficiency of the butyl rubber is rather poor. To overcome this problem, BIIR products that possess significantly higher reactivity are used. The higher reactivity is caused by the allylic bromide groups, which are sensitive to nucleophilic substitution with sulfur.<sup>25</sup> At the same time, these bromide groups are able to react with primary and secondary amines by an N-alkylation reaction offering the possibility of introducing various functionalities to BIIR.<sup>26</sup> On the basis of a study by Parent et al.,<sup>26</sup> we converted BIIR with butylimidazole at elevated temperatures (80–160 °C) in bulk. This reaction generates imidazolium bromide groups that we

assumed would form ionic associates. The reaction scheme is shown in Figure 2a. Before the actual reaction, isomerization of the allylic bromide groups from its exo-conformation to its endo-conformation, which is the reactive species in the system, is induced.<sup>27</sup> During the reaction, a distinct increase in the viscosity was observed within a short period of time, which made homogeneous mixing difficult. Therefore, the components were typically premixed in an internal mixer at 40 °C and then cured at higher temperatures under pressure. The curing process was monitored using moving die rheometer curves, as shown in Figure 2b,c. For comparison, pure BIIR was cured with sulfur according to a standard vulcanising recipe. At 100 °C, the curing curve of the butylimidazole BIIR mixture (Figure 2b) exhibited a continuous increase in elastic modulus, which exceeded the modulus of the sulfur-cured sample. This sulfur-cured sample was not fully cross-linked after curing at 100 °C. The curing curve of the butylimidazole BIIR mixture reveals effective cross-linking despite the absence of a cross-linking agent. The course of cross-linking observed is quite comparable to that of a diene rubber at higher temperatures. The fact that the butylimidazole-modified samples remained soluble after curing indicates that the cross-linking process is of a physical nature because of the ionic imidazolium bromide groups formed during the curing process. This assumption is supported by the rheometer curves recorded at different temperatures (Figure 2c). The highest elastic modulus was observed when the mixture was cured at 100 °C. The increasing curve progression suggests that cross-linking was not complete even after a 1 h of thermal treatment at 100 °C. The specific curve shape is most likely due to a dynamic ionic association process. During the entire curing time, ionic groups are successively formed, which contributes to the progressive formation of an ionic network. At higher temperatures, the

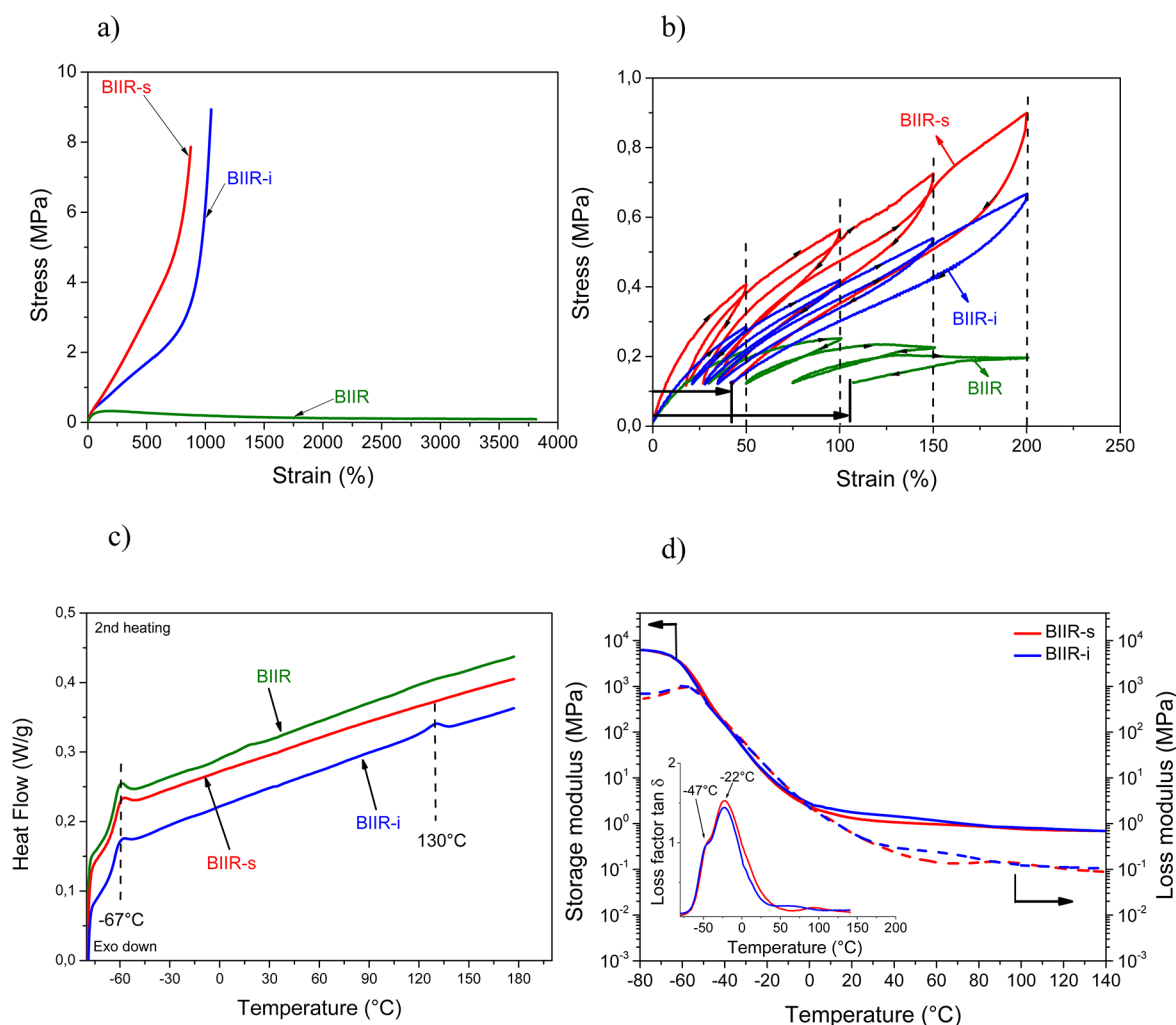


**Figure 3.** Mechanical and dynamic mechanical properties: (a) stress–strain plots; (b) mechanical responses to cyclic deformations; (c) DSC traces (second heating scan); and (d) DMA plots; imidazolium-modified BIIR (BIIR-i, blue), sulfur cross-linked BIIR (BIIR-s, red), and uncross-linked BIIR (green).

elastic modulus decreases, indicating that the ionic interactions gradually decrease with increasing temperature. This behavior is typical of imidazole-based ionomers. Low-molecular-weight derivatives of the latter are well-known to be ionic liquids that typically melt at temperatures less than 100 °C depending on their structure.<sup>28</sup> The reason for this behavior is the broad charge distribution within the conjugated organic molecule.

The degree of conversion was quantified by <sup>1</sup>H NMR spectroscopy. Details of this procedure are described in the Supporting Information (Figure S1). The conversion degree obtained at 80 °C is significantly lower (approximately 50%) than the expected maximum conversion degree based on the total amount of butylimidazole added. Almost complete conversion (approximately 90%) was observed at 100 °C or greater. To prevent loss of butylimidazole by evaporation and thermal decomposition of the rubber matrix, thermal treatment at temperatures substantially higher than 100 °C is typically avoided.

Next, the viscoelastic properties and self-healing behavior of the ionically modified BIIR, in which 74% of the bromine groups are converted using butylimidazole, are discussed. The properties are compared with those of the aforementioned sulfur-cured sample. When evaluating the sulfur-cured sample, we considered that the network density achieved by sulfur

cross-linking is limited because of the relatively low content of cross-linkable allylic bromide groups in BIIR. The conditions for sulfur cross-linking were optimized with regard to the maximum network density, and these details are presented in the Supporting Information (Figure S2). In the following discussion, the ionically modified and sulfur-modified BIIR are referred to as BIIR-i and BIIR-s, respectively.

Figure 3a,b show the stress–strain behavior of the imidazolium-modified BIIR compared to those of the sulfur cross-linked and uncross-linked BIIR. Notably, the properties of the ionically and sulfur cross-linked samples are typically consistent with each other. With 1000% stretchability and a tensile strength of 9 MPa, BIIR-i exhibited better tensile properties than BIIR-s (Figure 3a). A sharp bend in the curve for BIIR-i was clearly observed at 700–800% strain. This pronounced strain hardening is assumed to be the result of position changes and reorganizational processes of the ionic groups during stretching. Usually, strain hardening refers to the existence of covalent cross-linking points which more and more resist the force at higher strain. In BIIR-i, covalent cross-linking can be excluded since all samples are completely soluble in CHCl<sub>3</sub>. In our opinion, the stress–strain behavior can be explained by assuming that not all ionic groups are associated at the beginning of the experiment. This explains the moderate

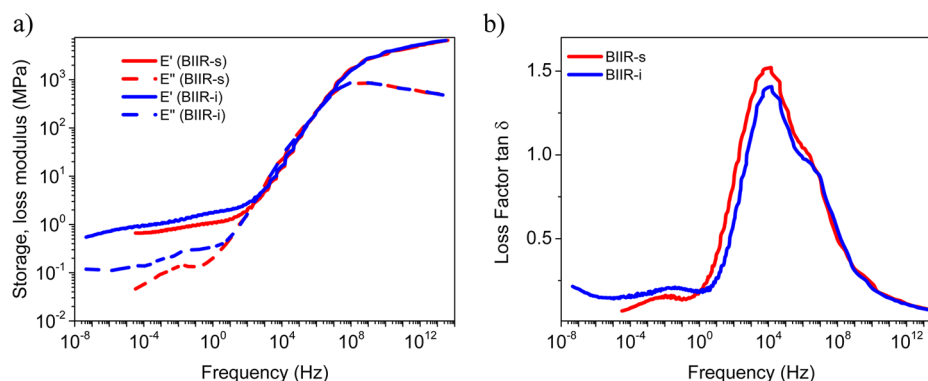


**Figure 4.** Frequency-dependent mechanical properties. Master curves of imidazolium-modified and sulfur cross-linked BIIR at a reference temperature  $T_{\text{ref}} = 20$  °C. (a) Frequency behavior of storage moduli  $E'$  and loss moduli  $E''$ . (b) Frequency behavior of the loss factors  $\tan \delta = E''/E'$ .

increase in stress at low strain. With increasing elongation, rearrangements take place which finally result in progressive association and formation of bigger ionic associates which act as cross-linking point similarly as covalent cross-links. In the covalently cross-linked network of BIIR-s, the rearrangements are limited to alteration of the chain conformations. As expected, the stress–strain properties of the uncross-linked BIIR are not significant.

Figure 3b shows the cyclic uniaxial stress–strain experiment with increasing maximum strains ( $\epsilon_{\text{max}} = 50, 100, 150,$  and  $200\%$ ). Both cross-linked samples exhibit typical stress softening (Mullin's effect) with hysteresis and permanent residual strain behavior.<sup>29,30</sup>

In every cycle, the stress-softening behavior is more prominent for the sulfur cross-linked sample because of the quasi-irreversible rearrangements of the monosulphidic, disulphidic, and poly sulphidic linkages during deformation.<sup>31</sup> Both BIIR-i and BIIR-s exhibit similar residual strain values (approximately 40%) after four cycles. However, the uncross-linked sample exhibited liquid-like behavior. In addition, a significantly smaller hysteresis loop was observed for BIIR-i compared with BIIR-s. This is attributable to the more elastic nature of the imidazolium-modified rubber, resulting from a different type of cross-linking caused by ionic association.

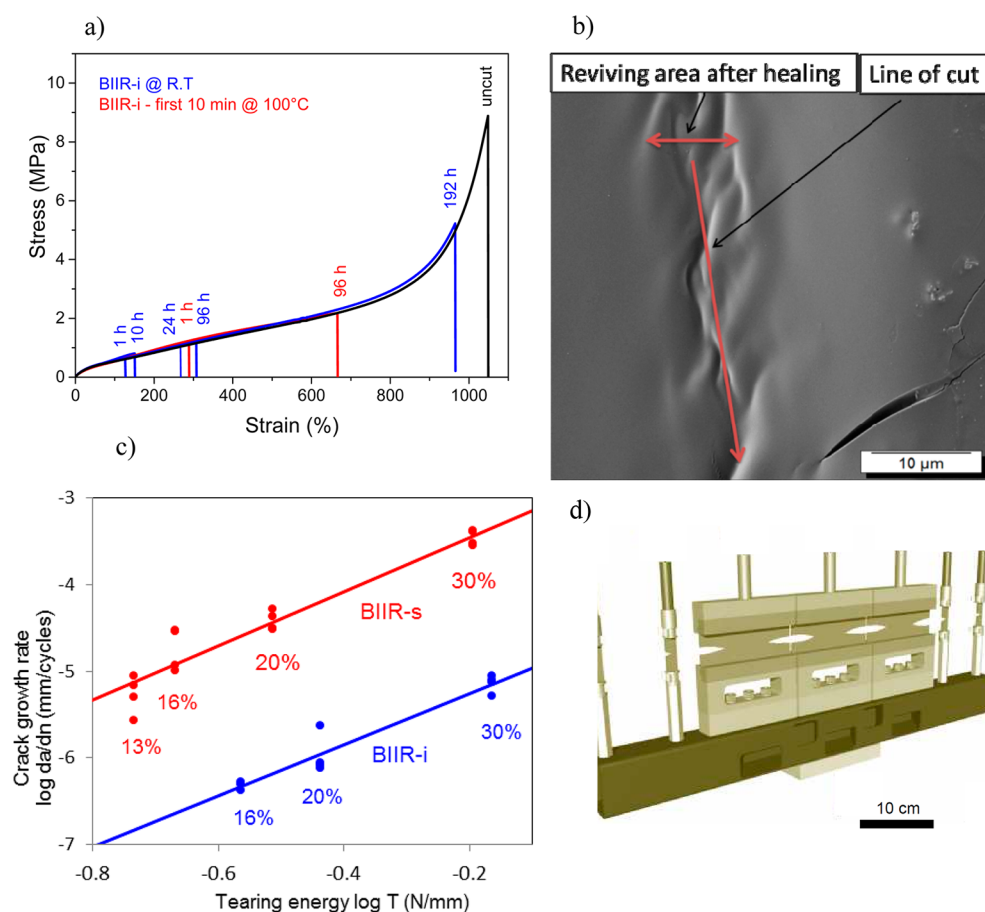
The presence of ionic associates was also supported by the thermal behavior of the rubber. Figure 3c shows the DSC heating curves of BIIR-i and BIIR-s. Both samples exhibited a glass-transition temperature ( $T_g$ ) of approximately  $-67$  °C. Additionally, the ionically modified BIIR-i exhibited an endothermic transition at  $130$  °C, which we interpret as melting of the ionic associates. This result is in good agreement with the observations made during the conversions of BIIR with butylimidazole (rheometric curves in Figure 2c), where decreasing elastic moduli were detected with increasing curing temperatures. Therefore, at higher temperatures, BIIR-i loses its network character.

Figure 3d shows the dynamic mechanical behavior of BIIR-s and BIIR-i. The viscoelastic spectrum ( $\tan \delta$  vs  $T$ ) of BIIR differs substantially from that of other amorphous polymers because of a very broad glass transition with a shoulder on the low-temperature side.<sup>32</sup> The maximum and shoulder are located at approximately  $-22$  and  $-47$  °C, respectively. Although the nature of the molecular mobility of butyl rubber remains unclear, the maximum peak may be due to Rouse modes dominating the viscoelastic response in the glass–rubber transition on the length scale of the entanglement spacing (i.e.,

in the case of the cross-linked or modified system, far below the spacing between two cross-links).<sup>32</sup>

The shoulder is due to sub-Rouse modes comprising approximately 10 backbone bonds. The plateau-like behavior at higher temperatures supports the assumed cross-linked network structures. At temperatures well above  $T_g$ , the storage modulus ( $E'$ ) exhibits a distinct rubbery plateau for both samples (Figure 3d), indicating considerable cross-linking of the rubbers.

Figure 4 compares the master curves for the storage and loss moduli as well as the loss factors of BIIR-s and BIIR-i at the reference temperature (i.e.,  $T_{\text{ref}} = 20$  °C). The master curves were based on the frequency sweep data from dynamic mechanical experiments at different temperatures and the application of the time–temperature superposition (TTS) principle according to the Williams–Landel–Ferry (WLF) model, which is similar to that previously described for ionic elastomers.<sup>33</sup> The TTS principle states that, as the temperature decreases, the shape of the relaxation curves remains the same but the characteristic relaxation time increases. Figure 4 shows the frequency behavior of the complex dynamic moduli of BIIR-s and BIIR-i; the results indicate that the dynamics of the underlying polymer networks are similar over a wide range of frequencies. Therefore, the recently introduced versatile multiscale approach (MSA) for the viscoelasticity of an unfilled rubber can be applied in both cases.<sup>28</sup> This MSA takes into account relaxation processes at different time and length scales and describes the dynamic moduli over nearly 16 frequency decades with a set of parameters, such as relaxation times and scaling exponents, that have a clear physical meaning.<sup>30</sup> Careful inspection and comparison of the corresponding curves in Figure 4 indicate small (height) differences in the low-frequency region (below  $\sim 10$  Hz). These differences are attributable to the different numbers and types of cross-links in BIIR-s (permanent sulfur bridges) and BIIR-i (ionic associate sizes). Within the MSA, for permanently and randomly cross-linked networks, the representation of the entangled dangling chains provides a plausible interpretation of the low-frequency constrained network dynamics and low-frequency scaling behavior (i.e.,  $E' \sim E'' \sim f^\alpha$ ). As a result, the scaling exponent ( $\alpha$ ) is a function of the degree of cross-linking, and its value is also influenced by the various mechanisms including the collective motion of network strands between junctions and the random connectivity of the network strands.<sup>34</sup> Therefore, the low-frequency scaling exponent ( $\alpha$ ) also depends on the specific nature of the cross-links. For BIIR-i, we assume that the



**Figure 5.** Self-healing behavior of ionically modified BIIR. (a) Stress–strain plots of mended samples of the imidazolium-modified BIIR after 1–192 h of healing at room temperature (blue). Some samples were maintained at 100 °C for the first 10 min of the total healing time (red). For comparison, the stress–strain plot of the uncut sample is shown (black). (b) Scanning electron micrograph showing the cut area after 24 h of healing at room temperature. (c) Crack growth rate as a function of tearing energy. The imidazole-modified rubber (BIIR-i, blue line) exhibits distinctly lower crack growth rates than the sulfur cross-linked one (BIIR-s, red line). The numbers indicate the percentage of the deformation amplitude. (d) Set-up of the tear fatigue analyzer (TFA) for the determination of the crack growth rate (the testing conditions are specified in the [Experimental Section](#)).

distribution of the ionic associate size and their inherent dynamics (appearance of co-operative motions) influence the cooperative low-frequency dynamics of the overall polymer network, leading to an increase in the loss modulus at lower frequencies as compared with the corresponding value for BIIR-s. As expected, the network dynamics at higher frequencies do not exhibit differences between the two types of rubbers.

In many respects, the property profile of the ionically cross-linked BIIR-i resembles that of a covalently cross-linked sample, particularly the properties at room temperature. However, owing to the presence of ionic groups, BIIR-i also exhibits some very interesting and unique features, which are manifested in a pronounced self-healing behavior. To illustrate this behavior, stress–strain measurements were performed on cut and restored BIIR-i samples (Figure 5a). The cut samples were allowed to heal at different temperatures and for different lengths of time. As the mending time increased, the healing effect increased, whereas the stress–strain paths after healing remain nearly unaffected. After 1 h of healing at room temperature, the mended sample exhibits an elongation at brake of 125%. After 192 h of annealing, the sample withstands a strain of 960% and a stress of 5.2 MPa (black curves). To increase the healing efficiency, the cut and restored sample was maintained at 100 °C for the first 10 min of the total healing

time (red curves). This procedure reduces the healing time significantly and results in comparable mechanical performance. After healing for 96 h (red curve in Figure 5a), the mended samples failed at a strain of 630%. This experiment is demonstrated in a supplementary movie (S3 and S4).

The origin of the self-healing behavior is obviously the ionic groups, the reversible interactions of which increase adhesion between the two cut pieces and hence compensate material damages. This is comparable with the mechanism described by Leibler et al. for a self-healing hydrogen bonded rubber.<sup>2</sup> In our system, reformation and growth of ionic associates in the interphase of the two cut pieces are assumed to be the reason for the self-healing effect observed. Such rearrangements are supported by the high intrinsic mobility of the isobutylene chains at ambient temperatures. This mobility ensures transport of still unassociated ionic groups or of already formed associates which grow after contact. The improved self-healing at elevated temperatures strongly supports this hypothesis. The higher chain mobility and reduced internal cohesion of the ionic associates facilitated the healing processes at elevated temperatures.

Notably, self-healing was observed at room temperature, which indicates that a certain degree of dynamic motion already exists and allows for rearrangement between the polymer chains

and ionic associates. A visual demonstration of the healing effect and the cutting line after 24 h of healing at room temperature are shown in Figure 5b. Between the two joined sections of the cut sample, a well-fused weld line with some wrinkle marks is visible. For the sake of completeness, the sulfur cross-linked BIIR-s do not exhibit self-healing behavior.

A cut rubber sample was used as an example of ultimate failure. In practice, rubber parts suffer from sporadic or periodic deformations at various strains and frequencies, resulting in the formation of microcracks that propagate, leading to failure of the material. A tear fatigue analysis (TFA) is performed to describe the failure behavior of a rubber material. Therefore, we studied and compared the crack growth behavior of notched specimens of BIIR-i and BIIR-s. The experiment was performed according to previously published protocols.<sup>23,24</sup> The relationship between stable crack growth rate and the tearing energy follows the Paris-Erdogan power law (with exponent  $m$ ), which is expressed as  $da/dn = T^m$ , where  $a$  is the crack length,  $n$  is the number of deformation cycles, and  $T$  is the tearing energy. Figure 5c shows the results of the TFA of BIIR-i and BIIR-s. At a certain tearing energy, the crack growth rate ( $da/dn$ ) for BIIR-i is much lower compared with that of BIIR-s. Due to the presence of ionic associates in the modified rubber, the crack propagation rate may be significantly smaller. The ionic associates present in the crack tip may dissociate into smaller aggregates that are not completely destroyed. In addition, ion hopping during elongation may facilitate further reaggregation or reassociation of the ionic groups, leading to a higher crack resistance. A similar effect was observed when the rubber was reinforced with fillers, such as carbon black or silica. With respect to the fracture mechanical properties, the imidazole-modified BIIR behaves like a filled rubber composite despite the absence of any filler particles.

## CONCLUSIONS

Isoprene–isobutylene copolymers behave like a cross-linked rubber after imidazole modification. The study shows that modification of the chemical group of bromine containing rubber can allow preparing elastomeric rubber composites without the use of conventional sulfur or peroxide. The ionic association mediated cross-linking can offer superior overall performance of the materials and even self-repairing effect can be realized. Direct visualization of self-healing character by scanning electron microscopy and the alteration of the viscoelastic behavior of the modified rubber by different mechanical analysis were realized in this report. Fracture mechanical studies directly provide evidence of superior tear fatigue properties for the modified BIIR. The development of the cross-linking nature of the rubbers without further use of cross-linking chemicals also reduces the number of rubber processing steps. The concept of this self-healing approach could be applied to other halide-containing polymers. In addition to easy processing, these materials also have unique advantages over the conventional rubbers as they do not need any curatives or cross-linking agents. Furthermore, this material could be compounded with conventional fillers such as carbon black and silica for strength enhancement of the materials, if necessary. The imidazole modified elastomer presented in this work offers the versatility to the materials scientists to exploit these products as a commercial commodity for rubber parts. Ease of processing and absence of nontoxic vulcanizing chemicals to synthesize such novel self-healing rubbers opens a new horizon in rubber technology.

Finally, the present work is a sound contribution to understand the self-healing behavior of imidazole modified rubber. Though no direct experimental evidence has been put forward to confirm the assumed rearrangements of the ionic groups at the place of damage, the total sum of results strongly supports the proposed mechanism of self-healing. This novel approach, from both the materials and processing points of view, may significantly increase interest in both commercial application and academic research.

## ASSOCIATED CONTENT

### Supporting Information

The Supporting Information is available free of charge on the ACS Publications website at DOI: 10.1021/acsami.5b05041.

<sup>1</sup>H NMR spectra (CDCl<sub>3</sub>) of bromobutyl rubber and bromobutyl rubber converted with butyl imidazole at 100 °C. Rheometer curves of BIIR-s compounded with different amount of sulfur. Stress–strain curves obtained from sulfur vulcanized BIIR with different amounts of sulfur. (PDF)

Stress–strain experiment of the mended sample using a Zwick tensile tester. (AVI)

Stress–strain experiment of the mended sample using a manual stretching device. (AVI)

## AUTHOR INFORMATION

### Corresponding Author

\*E-mail: das@ipfdd.de.

### Notes

The authors declare no competing financial interest.

## ACKNOWLEDGMENTS

This work was supported by the Deutsche Forschungsgemeinschaft (DFG) in the Priority Program (Schwerpunktprogramm, SPP 1568) “Design and Generic Principles of Self-Healing Materials”. The authors thank K. Saalwächter for fruitful discussions.

## REFERENCES

- (1) Mihashi, H.; Nishiwaki, T. Development of Engineered Self-healing and Self-Repairing Concrete-state-of-the-art Report. *J. Adv. Concr. Technol.* **2012**, *10*, 170–184.
- (2) Cordier, P.; Tournilhac, F.; Soulié-Ziakovic, C.; Leibler, L. Self-healing and Thermoreversible Rubber from Supramolecular Assembly. *Nature* **2008**, *451*, 977–980.
- (3) Ahn, K. B.; Lee, D. W.; Israelachvili, J. N.; Waite, J. H. Surface-initiated Self-healing of Polymers in Aqueous Media. *Nat. Mater.* **2014**, *13*, 867–872.
- (4) Montarnal, D.; Tournilhac, F.; Hidalgo, M.; Couturier, J. L.; Leibler, L. Versatile One-pot Synthesis of Supramolecular Plastics and Self-healing Rubbers. *J. Am. Chem. Soc.* **2009**, *131*, 7966–7967.
- (5) Colquhoun, H. M. Self-repairing polymers: Materials that Heal Themselves. *Nat. Chem.* **2012**, *4*, 435–436.
- (6) Burnworth, M.; Tang, L.; Kumpfer, J. R.; Duncan, A. J.; Beyer, F. L.; Fiore, G. L.; Rowan, S. J.; Weder, C. Optically Healable Supramolecular Polymers. *Nature* **2011**, *472*, 334–337.
- (7) Wietor, J. L.; Sijbesma, R. P. A Self-healing Elastomer. *Angew. Chem., Int. Ed.* **2008**, *47*, 8161–8163.
- (8) Chen, Y.; Kushner, A. M.; Williams, G. A.; Guan, Z. Multiphase Design of Autonomic Self-healing Thermoplastic Elastomers. *Nat. Chem.* **2012**, *4*, 467–472.
- (9) Blaiszik, B. J.; Kramer, S. L. B.; Olugebefola, S. C.; Moore, J. S.; Sottos, N. R.; White, S. R. Self-healing Polymers and Composites. *Annu. Rev. Mater. Res.* **2010**, *40*, 179–211.

- (10) Syrett, J. A.; Remzi Becer, C.; Haddleton, D. M. Self-healing and Self-mendable Polymers. *Polym. Chem.* **2010**, *1*, 978–987.
- (11) Wool, R. P. Self-healing Materials: A Review. *Soft Matter* **2008**, *4*, 400–418.
- (12) Keller, M. W.; White, S. R.; Sottos, N. R. A Self-healing Poly (Dimethyl Siloxane) Elastomer. *Adv. Funct. Mater.* **2007**, *17*, 2399–2404.
- (13) Wu, D. Y.; Meure, S.; Solomon, D. Self-healing Polymeric Materials: A Review of Recent Developments. *Prog. Polym. Sci.* **2008**, *33*, 479–522.
- (14) Maes, F.; Montarnal, D.; Cantournet, S.; Tournilhac, F.; Corté, L.; Leibler, L. Activation and Deactivation of Self-healing in Supramolecular Rubbers. *Soft Matter* **2012**, *8*, 1681–1687.
- (15) Herbst, F.; Binder, W. H. Self-healing Polymers via Supramolecular, Hydrogen-Bonded Networks. In *Self-Healing Polymers: From Principles to Applications*, 1st ed.; Binder, W. H., Ed.; ISBN: 978-3-52733439-1; Wiley-VCH Verlag GmbH & Co. KGaA: Weinheim, pp 275–300, 2013.
- (16) Parent, J. S.; Malmberg, S. M.; Whitney, R. A. Auto-catalytic Chemistry for the Solvent-free Synthesis of Isobutylene-rich Ionomers. *Green Chem.* **2011**, *13*, 2818–2814.
- (17) Hohlbein, N.; Pelzer, T.; Nothacker, J.; Von Tapavicza, M.; Nellesen, A.; Datta, H.; Schmidt, A. M. Self-healing Processes in Ionomeric Elastomers. In *ICHM 2013: Proceedings of the 4th International Conference on Self-Healing Materials*, Ghent, Belgium, June 16–20, 2013, Ghent University, Ghent, Belgium, 2013. ISBN: 9789082073713..
- (18) Rahman, Md A.; Sartore, L.; Bignotti, F.; Di Landro, L. Autonomic Self-healing in Epoxidized Natural Rubber. *ACS Appl. Mater. Interfaces* **2013**, *5*, 1494–1502.
- (19) Wang, D.; Guo, J.; Zhang, H.; Cheng, B.; Shen, H.; Zhao, N.; Xu, J. Intelligent Rubber with Tailored Properties for Self-healing and Shape Memory. *J. Mater. Chem. A* **2015**, *3*, 12864.
- (20) Schüssele, A. C.; Nübling, F.; Thomann, Y.; Carstensen, O.; Bauer, G.; Speck, T.; Mühlaupt, R. Self-healing rubbers based on NBR blends with hyperbranched Polyethylenimines. *Macromol. Mater. Eng.* **2012**, *297*, 411–419.
- (21) Stephen, J.; Kalista, Jr. Self-Healing Ionomers. In *Self-Healing Materials: Fundamentals, Design Strategies, and Applications*, 1st ed.; Ghosh, S. K., Eds.; ISBN: 978-3-527-31829-2; Wiley-VCH Verlag GmbH & Co. KGaA: Weinheim, 2008; pp 73–97.
- (22) Varley, R. J.; van der Zwaag, S. Development of a Quasi-static Test Method to Investigate the Origin of Self-healing in Ionomers under Ballistic Conditions. *Polym. Test.* **2008**, *27*, 11–19.
- (23) Stoček, R.; Heinrich, G.; Gehde, M.; Kipscholl, R. Analysis of Dynamic Crack Propagation in Elastomers by Simultaneous Tensile- and Pure-shear-mode Testing. In *Fracture Mechanics and Statistical Mechanics of Reinforced Elastomeric Blends*, 1st ed.; Grellmann, W.; Heinrich, G.; Kaliske, M.; Klüppel, M.; Schneider, K.; Vilgis, T., Eds.; ISBN 978-3-642-37910-9; Springer-Verlag: Berlin, Heidelberg, 2013; pp 269–301.
- (24) Stoček, R.; Heinrich, G.; Gehde, M. A New Testing Concept for Determination of Dynamic Crack Propagation in Rubber Materials. *Kautsch. Gummi Kunstst.* **2012**, *9*, 49–53.
- (25) Röthemeyer, F.; Sommer, F.; *Kautschuk Technologie*; 3rd ed.; ISBN: 978-3-446-43776-0; Carl Hanser Verlag: München, 2013.
- (26) Parent, J. S.; Porter, A. M. J.; Kleczek, M. R.; Whitney, R. A. Imidazolium Bromide Derivatives of Poly (isobutylene-co-isoprene): A New Class of Elastomeric Ionomers. *Polymer* **2011**, *52*, 5410–5418.
- (27) Malmberg, S. M.; Parent, J. S.; Pratt, D. A.; Whitney, R. A. Isomerization and Elimination Reactions of Brominated Poly (isobutylene-co-isoprene). *Macromolecules* **2010**, *43*, 8456–8461.
- (28) Huddleston, J. G.; Visser, A. E.; Reichert, W. M.; Willauer, H. D.; Broker, G. A.; Rogers, R. D. Characterization and Comparison of Hydrophilic and Hydrophobic Room Temperature Ionic Liquids Incorporating the Imidazolium Cation. *Green Chem.* **2001**, *3*, 156–164.
- (29) Mullins, L.; Tobin, N. R. Theoretical Model for the Elastic Behavior of Filler-Reinforced Vulcanized Rubbers. *Rubber Chem. Technol.* **1957**, *30*, 555–571.
- (30) Schmoller, K. M.; Bausch, A. R. Similar Nonlinear Mechanical Responses in Hard and Soft Materials. *Nat. Mater.* **2013**, *12*, 278–281.
- (31) Morrison, N. J.; Porter, M. Temperature Effects on the Stability of Intermediates and Crosslinks in Sulfur Vulcanization. *Rubber Chem. Technol.* **1984**, *57*, 63–85.
- (32) Wu, J.; Huang, G.; Pan, Q.; Zheng, J.; Zhu, Y.; Wang, B. An Investigation on the Molecular Mobility through the Glass Transition of Chlorinated Butyl Rubber. *Polymer* **2007**, *48*, 7653–7659.
- (33) Basu, D.; Das, A.; Stöckelhuber, K. W.; Jehnichen, D.; Formanek, P.; Sarlin, E.; Vuorinen, J.; Heinrich, G. Evidence for an In-situ Developed Polymer Phase in Ionic Elastomers. *Macromolecules* **2014**, *47*, 3436–3450.
- (34) Grenzer, M.; Toshchevnikov, V.; Gazuz, I.; Petry, F.; Westermann, S.; Heinrich, G. Multiscale Approach to Dynamic-mechanical Analysis of Unfilled Rubbers. *Macromolecules* **2014**, *47*, 4813–4823.